# STORAGE OF VERY COLD NEUTRONS IN A TRAP WITH NANO-STRUCTURED WALLS

E. V. Lychagin[1], A. Yu. Muzychka[1], G. V. Nekhaev[1], V. V. Nesvizhevsky[2], G. Pignol[3], K. V. Protasov[3], A. V. Strelkov[1]

[1]JINR, 6 Joliot-Curie, Dubna, Moscow reg., Russia, 141980
[2]ILL, 6 rue Jules Horowitz, Grenoble, France, F-38042
[3]LPSC (UJF, CRNS/IN2P3, INPG), 53, rue des Martyrs, Grenoble, France, F-38026

**Abstract**
We report on storage of Very Cold Neutrons (VCN) in a trap with walls containing powder of diamond nanoparticles. The efficient VCN reflection is provided by multiple diffusive elastic scattering of VCN at single nanoparticles in powder. The VCN storage times are sufficiently long for accumulating large density of neutrons with complete VCN energy range of up to a few times $10^{-4}$ eV. Methods for further improvements of VCN storage times are discussed.

**Keyword**
Very cold neutrons; diamond nanoparticles; neutron scattering; fundamental particle physics.

## Introduction

Recently we showed that powders of nanoparticles could be used efficiently as first reflectors of Very Cold Neutrons (VCN) in velocities range up to 160 m/ [1], thus bridging the energy gap between efficient reactor reflectors [2] for thermal and cold neutrons, and effective Fermi potential for ultracold neutrons (UCN) [3].

The possibility to use medium with nanoparticles like a reflector of VCN has been treated in [4]. If a neutron comes in such a medium then its velocity direction changes many times due to scattering on the particles. In the issue neutron can live this medium back. In other words, the neutron is reflected from the medium. In [4] was shown that the reflector is more effective if the particles size is close to the neutron wavelength. A large number of diffusive collisions needed to reflect VCN from powder constrains the choice of materials: only low-absorbing ones with high effective Fermi potential are appropriate. Thus, diamond nanoparticles were an evident candidate for such VCN reflector. The formation of diamond nanoparticles by explosive shock was first observed more than forty years ago [5]. Since then very intensive studies of their production and of their various applications have been performed worldwide. These particles measure a few nanometers; they consist of a diamond nucleus (with a typical diamond density and Fermi quasipotential) within an onion-like shell with a complex chemical composition [6] (with lower Fermi quasipotential). A recent review of the synthesis, structure, properties and applications of diamond nanoparticles can be found in [7].

The first experiments on the reflection of VCN from nano-structured materials as well as on VCN storage were carried out in the seventies in [8] and later continued in [9]. In [1] we extended significantly the energy range and the efficiency of VCN reflection by exploiting diamond nanoparticles. A reflector of this type is particularly useful for both UCN sources using ultracold nanoparticles [4, 10] and for VCN sources; it would not be efficient however for cold and thermal neutrons, as shown in [11].

In order to measure precisely the VCN reflection probability from powder of diamond nanoparticles and to explore feasibility of VCN storage in traps with nano-structured walls, we carry out a dedicated experiment described in the present article. In fact, the measuring procedure used here is equivalent to that typically used in experiments on UCN storage in traps (see for example [12, 13]). The difference consists in a type of trap walls and in characteristic values of the reflection probability.

**The experimental setup**

This experiment was carried out at the VCN beam, PF2, ILL. The installation scheme is shown in Fig. 1.

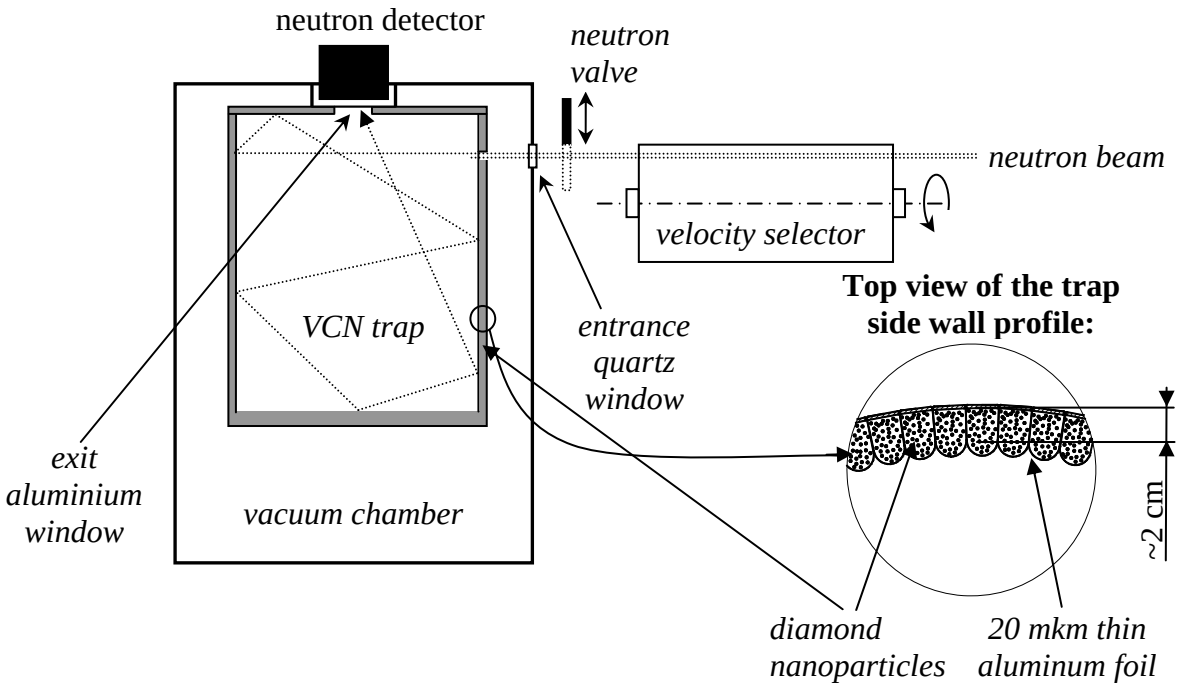


Fig.1 The installation scheme.

The VCN trap has cylindrical shape with a diameter of 44 cm and a height of 47 cm. VCN could enter the trap through a small square window of 2 cm by 2 cm in its side wall. The VCN beam diameter is ~1 cm. VCN could be reflected many times from the trap walls. Thus they could find an exit circular window with a diameter of 6~cm in the trap cover and enter into a detector behind the window. The VCN beam could be opened or closed using a fast cadmium valve with a thickness of 0.2 mm. The VCN velocity could be chosen using a velocity selector in front of the valve. The trap is placed inside a vacuum chamber with an entrance quartz window with a thickness of 3 mm and an exit aluminum window with a thickness of 1 mm. When the VCN beam is closed the detector count rate decreases exponentially following the VCN density in the trap. Thus we could measure the VCN storage times as a function of their velocity.

The neutron detector is a gaseous proportional $^3$He counter (the thickness of its sensitive layer is 5 cm, the $^3$He partial pressure is 200 mbar) with an entrance aluminum window with a thickness of 100 μm and a diameter of 9 cm. The electrical detector signals are analyzed using the time and amplitude information.

The velocity selector consists of a cylinder with a length of $l$=40 cm and a diameter of $D$=19 cm. Curved plastic plates with a thickness of 1 mm are installed at the side surface of the cylinder in such a way that they form screw-like slits with a width of $d$ ~4.5 mm and the screw length of $L$=480 cm. The cylinder rotates around its axis with the period T. Neutrons could scatter at hydrogen atoms in the plate's material; those neutrons leave the neutron beam. The rotation period defines the velocity of neutrons passing through the selector. Neutrons with low angular divergence and with momentum parallel to the selector axis pass through the selector screw slits, thus avoiding scattering by the plates only if the neutron velocity is equal to:

$$v = L\frac{2\pi}{T}\left(1 \pm \frac{dL}{2\pi Dl}\right).$$

The selector allowed us to choose the neutrons with a velocity in the range of 30-160 m/s. The velocity resolution was measured using time-of-flight method; the some results are shown in Fig. 2.

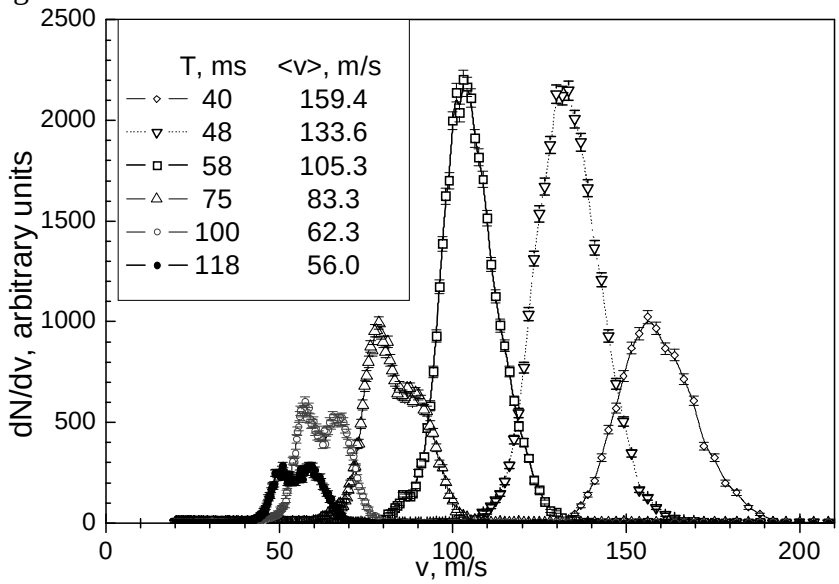


Fig. 2 Experimental time-of-flight neutrons spectra after the velocity selector are presented (neutron chopper resolution is different for various curves). Labels at the figure indicate the rotation period of the velocity selector and average velocity in the spectra.

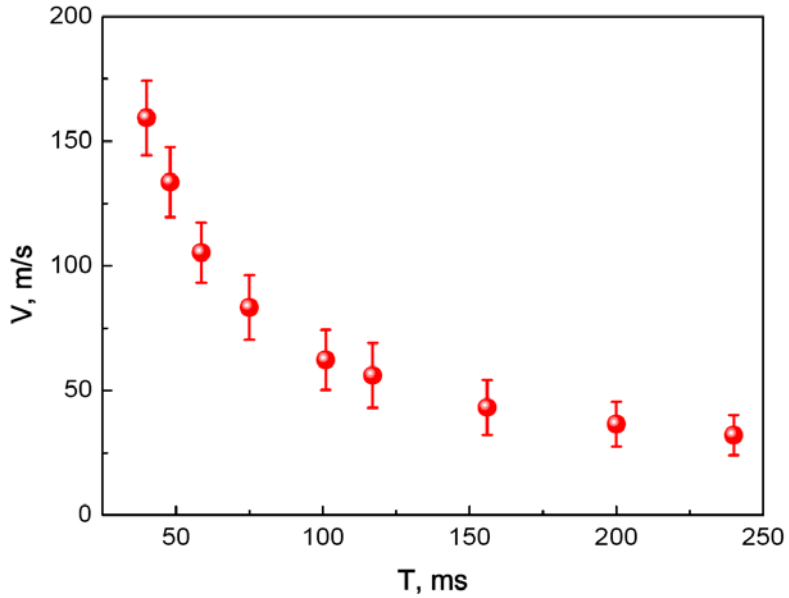


Fig. 3 The neutron average velocities at the velocity selector exit are shown as a function of its rotation period. Error bars indicate the half width of velocity distribution in the beam after selector (because these distributions are not Gaussians).

Fig. 3 summarizes the time-of-flight measurements results. It presents neutrons average velocity at the velocity selector exit as a function of its rotation period. Error bars indicate the half width of velocity distribution in the beam after selector. Neutron chopper resolution has been took into account and subtracted.

The neutron flux at the selector exit is shown in Fig. 4.

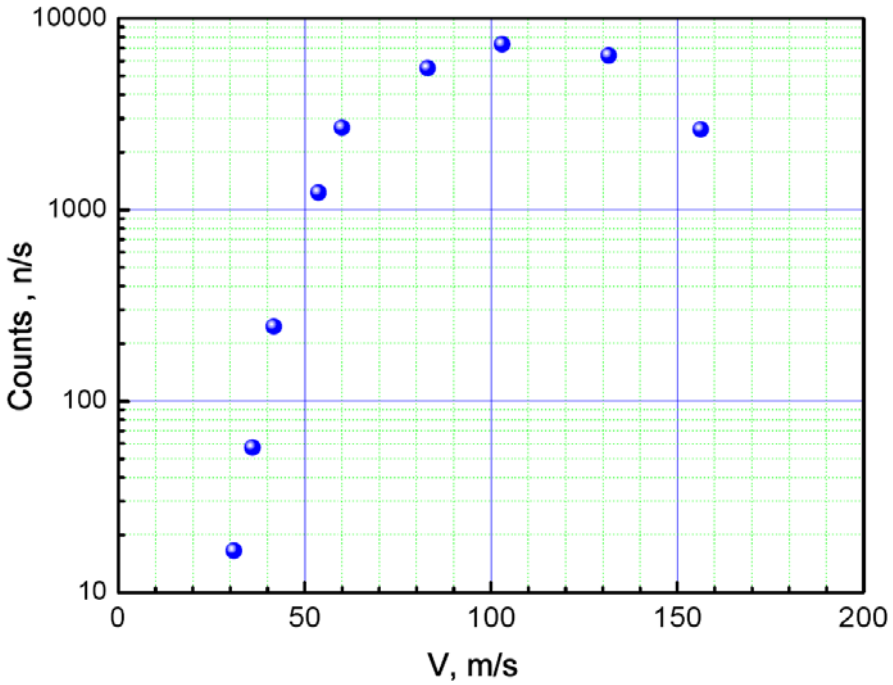


Fig. 4 The neutron flux at the selector exit is shown as a function of neutron velocity

The valve is controlled by an electro-magnet governed with an electric pulse generator. The time of opening and closing the valve was measured in a separate experiment with a light beam; it is equal to 5 ms in both cases.

The trap is built using powder of diamond nanoparticles. To build the trap side walls from the powder we decided to fill nanoparticles into aluminum tubes, and to assemble them into a cylinder as shown in Fig. 1 and in Fig. 5. Thus the walls are not quite homogeneous. VCN reflect many times from the trap walls, thus they pass many times through aluminum walls of the tubes. In order to avoid significant losses of VCN in aluminum, we have to decrease the aluminum wall thickness to a minimum value. Therefore the tubes are built using 20 μm thick aluminum foil. We fill in the tubes with powder and compressed it. The compressed powder density is 0.4 g/cm$^3$. The trap cover is shown in Fig. 6. It was design like a tambourine with height of 3 cm and 30 μm thickness aluminum foil membrane. This "tambourine" is filled by powder with density of 0.3 g/cm$^3$. A window in the cover center (see Fig. 6) allows us to count VCN in the detector. The cover is installed on top of the trap side wall; thus an eventual slit between the side wall and the cover surface is minimized. The trap bottom is covered with powder with a thickness of 3 cm compressed to a density of 0.3 g/cm$^3$.


Fig. 5 The VCN trap. The cover is open.

Fig 6 The cover with a window in its center.

Electro-heaters are rolled around the trap; the trap and the electro-heaters are covered by many aluminum foil layers in order to provide thermal isolation of the trap. The trap temperature could be raised using the electro-heaters and measured with two thermo-pairs attached to the massive aluminum parts of the trap bottom and the cover respectively.

**The experimental results**

When the valve is open VCN fill in the trap as long as needed to reach a saturation VCN density. Then we close the valve and measure the time constant of the exponential decrease of the VCN density in the trap. The detector count rate is proportional to the VCN density in the

trap. Such a measuring cycle is repeated many times in order to accumulate sufficient statistics.

An example of the neutron count rate during one cycle is shown in Fig. 7; a background is subtracted. The solid line in Fig. 7 shows the light signal, in arbitrary units, used to synchronize the valve with the measuring cycle. A pulse generator starts the cycle at time $t$=0, opens the valve at $t$=50 ms, and closes the valve at $t$=250 ms. When the valve is open the trap could be filled in with VCN up to a saturation density. When the valve is closed, the VCN density decreases exponentially. The characteristic time of this decrease is equal to a convolution of the VCN storage time and empting time. The dominant loss factor is associated with the trap walls, as the area of the entrance and exit windows is smaller than 0.3% compared to total area of the trap surface. The storage time in Fig. 7 is equal to $\tau_{st}^{VCN} = (19.0 \pm 0.5)$ ms.

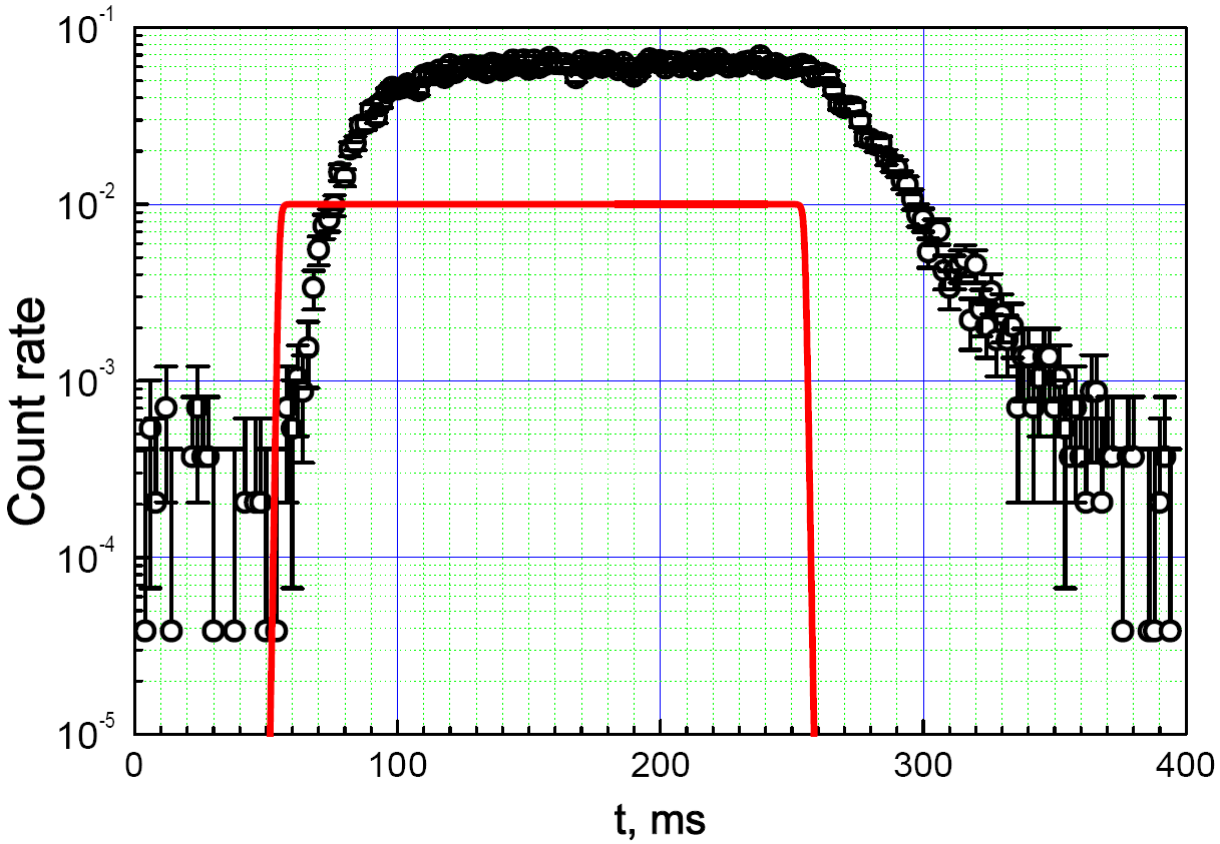


Fig. 7 An example of the neutron count rate during a measurement cycle for the VCN velocity of 85 m/s. The solid line shows the light signal, in arbitrary units, used to synchronize the valve with the measurement cycle.

Analogous measurements were carried out for this and other VCN velocities in 3 series of measurements. First, we pumped out the trap during 12 hours then measured the VCN storage times at room temperature. Second, the vacuum chamber was filled in with argon at a pressure of 1 bar then the trap was heated to a temperature of ~ 120ºC and kept at this temperature during 3 hours. After that argon was pumped out, the trap was slowly cooled to a room temperature then VCN storage times were measured. Third, we heated the trap to a temperature of ~145ºC on permanent pumping. The measurement started when the temperature (measured with the two termo-pairs) had got stabilized. Besides, the detector

count rate (with the valve open and the neutron velocity equal to 160 m/s) had to get stabilized as well. The later process is delayed because of slow heating of internal zones of powder.

The results of all these 3 series of measurements are shown in Fig. 8. Storage times were not measured for fast neutrons in the third series, because they are too short.

As it possible to see from the Fig. 8 the degassing of the trap not leads to increasing of the neutron storage time to compare with the pumped trap. Though increasing the trap temperature up to 150°C (30% in absolute scale) has led to decreasing of neutron storage time at 30% approximately. It looks like increasing of neutron losses due to inelastic scattering by hydrogen bounded strongly (it is not removed by 150°C degassing) to the diamond.

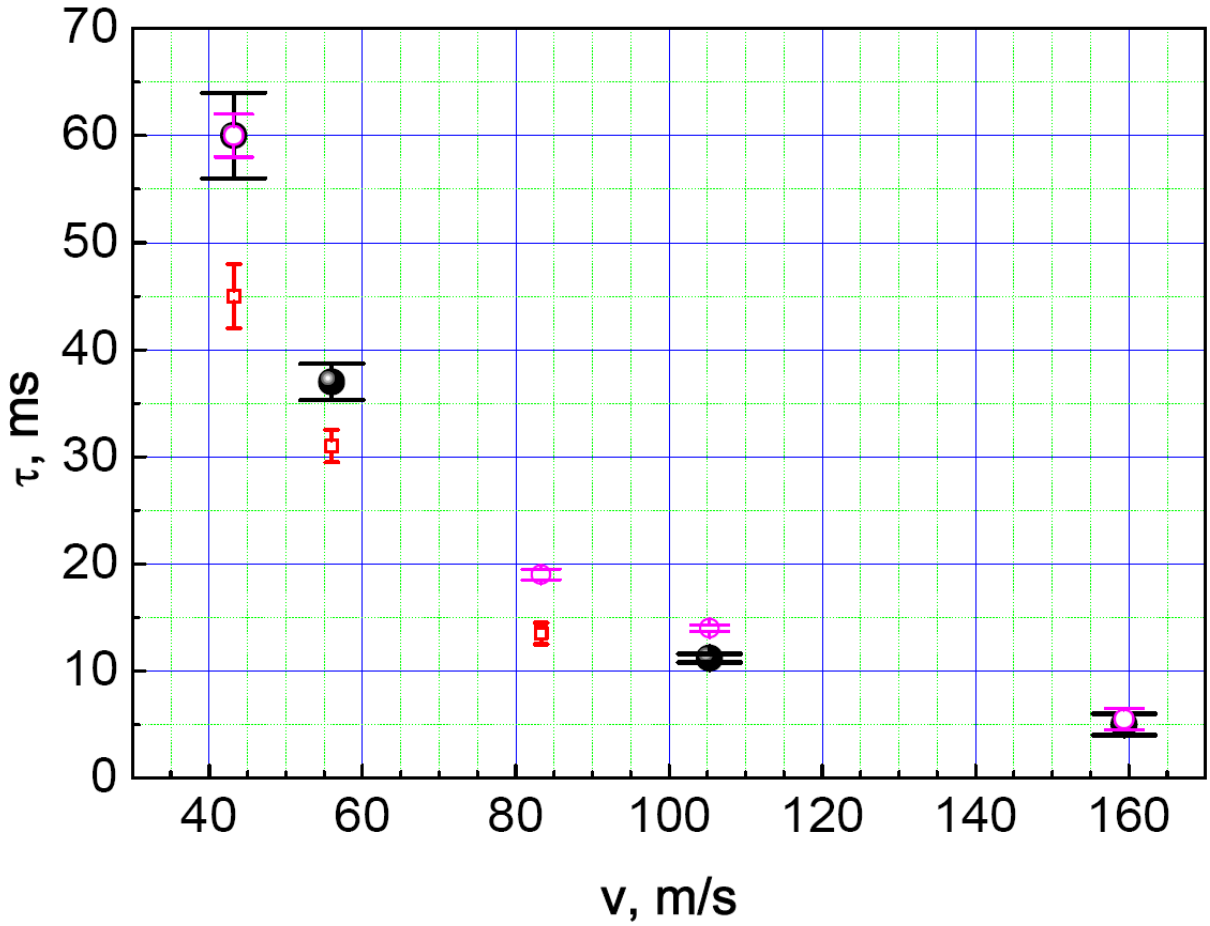


Fig. 8 The VCN storages times as a function of their velocity. Black circles correspond to measurements at room temperature after 12 hour pumping. Empty circles show measurements at room temperature after heating the trap at 120ºC in argon. Boxes indicate results obtained at a temperature of 150ºC under permanent pumping.

**Analysis of the experimental results**

For the trap geometry described above we calculate a VCN mean free path for all neutron velocities :

$\Delta x = 22 \pm 1\, cm$

neglecting small gravitational corrections. Thus the probability of VCN reflection from the trap wall could be estimated from equation:

$$P(v) = 1 - \frac{\Delta x}{\tau_{st}^{VCN}(v) \cdot v} \cdot (1 - \varepsilon) \qquad (1)$$

where $\varepsilon$ accounts for VCN losses in the entrance and exit windows and amounts to $\varepsilon$=3.5·10$^{-3}$. The errors in this estimation are defined by storage time uncertainty (see Fig. 8), mean flight pass uncertainty and neutron velocity uncertainty (see Fig. 3).

This probability represents the reflectivity for the walls actually used in this experiment. It thus includes losses in the aluminium foil, and effects of the geometrical shape of the trap walls. This estimation supposes isotropic angle distribution of neutrons in the trap that is not quite true for more fast neutrons.

On the other hand, we have in hand a model for the propagation of neutrons in the nanoparticle powder. The method used here to describe the reflection of VCN at a layer of nanoparticles is similar to that in [1]. Namely, we neglected the relatively complex internal structure of the nanoparticle and modeled it as a uniform sphere. The neutron-nanoparticle elementary interaction was calculated using the first Born approximation. The amplitude for a neutron with the energy $(\hbar k)^2/2m$ to be scattered at a spherical nanoparticle with the radius *R* and Fermi potential *V*, at an angle $\theta$ is equal:

$$f(\theta) = -\frac{2m}{\hbar^2} VR^3 \left( \frac{\sin(qR)}{(qR)^3} - \frac{\cos(qR)}{(qR)^2} \right),$$

where $q = 2k\sin(\theta)$ is the transferred momentum. The total elastic cross section is equal correspondingly:

$$\sigma_s = \int |f|^2 d\Omega = 2\pi \left| \frac{2m}{\hbar^2} V \right|^2 R^6 \frac{1}{(kR)^2} I(kR),$$

where

$$I(kR) = \frac{1}{4}\left( 1 - \frac{1}{(2kR)^2} + \frac{\sin(4kR)}{(2kR)^3} - \frac{\sin^2(2kR)}{(2kR)^4} \right).$$

The chemical composition of the nanoparticle is complex and includes carbon (up to 88% of the total mass), hydrogen (1%), nitrogen (2.5%), oxygen (up to 10%) [14]. Moreover, a certain amount of water covers a significant surface area of the nanoparticles. In general, the hydrogen in the water and on the surface of the nanoparticles scatters the neutrons up to the thermal energy range (*up-scattering*); thermal neutrons do not interact as efficiently with nanoparticles and therefore traverse powder. The hydrogen quantity in the powder was measured by (n,γ) method and composition $C_{15}H$ was found for degassed and non degassed powder in the vacuum and composition $C_8H$ was found for powder in the air.

To compare the experimental results to the model of independent nanoparticles, we further corrected the measured reflectivity from VCN loss in aluminum foils and from a dead zone in the wall structure in between each cylinder (this correction is about 1%). The corrected reflectivity is shown in Fig. 9 for measurements at room temperature (averaged through two series of measurements); together with the Monte-Carlo calculation. The only parameter of this calculation concerns inelastic scattering on hydrogen. In the Monte-Carlo simulation, the quantity of hydrogen is fixed according to the $C_{15}H$ chemical composition (0.5% of the total mass). Besides, the cross section for inelastic scattering is assumed to follow the 1/v rule, and the value of the cross section $\sigma_H$ for neutron velocity of 2200 m/s is considered as an effective parameter. The calculation reproduces the velocity dependance of the reflectivity well, and the effective parameter is fitted at the approximate value of $\sigma_H$ = 1.3 barn.

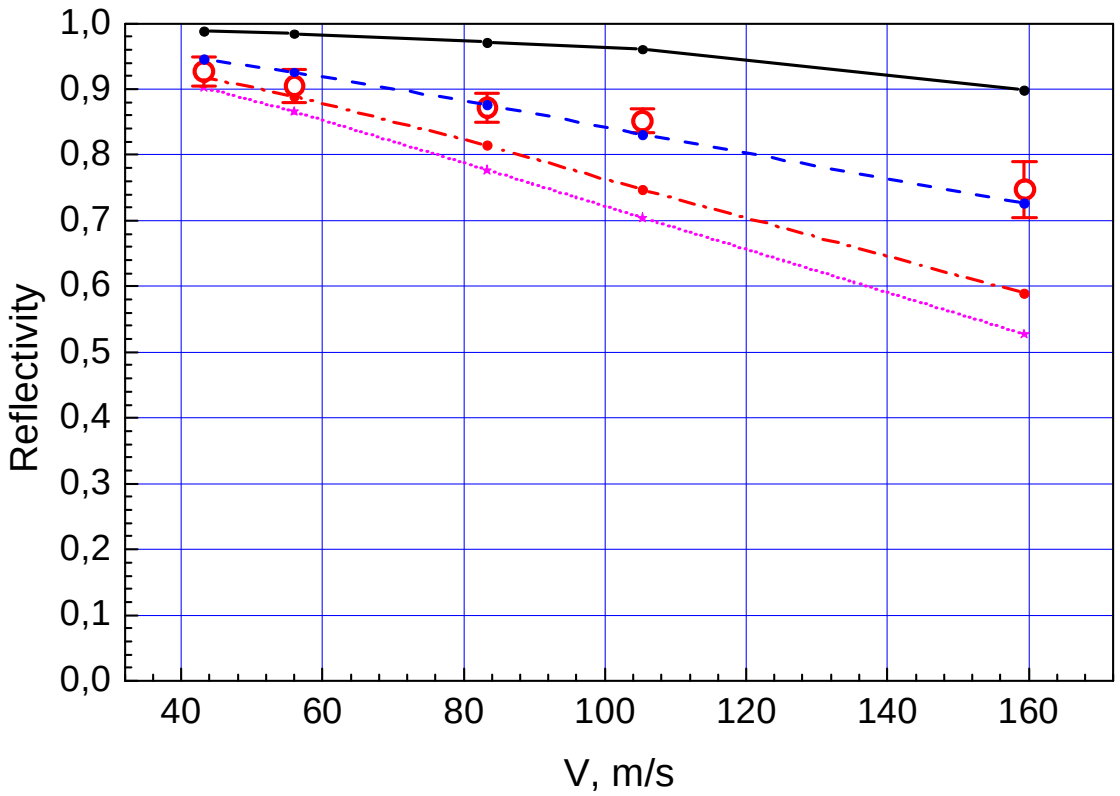


Fig. 9 The probability of VCN reflection from a layer of nanoparticles as a function of their velocity. Open circles correspond to measurements at room temperature. Thin lines correspond to Monte-Carlo calculations, taking into account capture and upscattering at hydrogen, the quoted cross section corresponds to neutron velocity of 2200 m/s: 4 barn for dotted line, 3 barn for dot-dashed line, 1.3 barn for dashed line and 0 barn for plain black line.

**Conclusion**

We have observed for the first time storage of VCN with the velocity 40-160 m/s (the energy up to $10^{-4}$ eV) in a trap with walls containing powder of diamond nanoparticles. The VCN storage will allow us to accumulate significant number (density) of VCN in a trap (much larger than that typical for UCN). Further improvement of the VCN storage times could be achieved by removing a part of hydrogen from powder (it could not be removed by degassing at 150°C) to suppress inelastic up-scattering of VCN. Another option could consist in replacing the diamond nanoparticles by $O_2$, $D_2$, $D_2O$, $CO_2$, CO or other low-absorbing nanoparticles, free of hydrogen and other impurities with significant VCN loss cross-section.

The probability of cold neutron isotropic flux reflection from diamond nano particles is compared with others well know reflectors in Fig. 11. As it can be seen from Fig. 10, the maximum energy of the reflected VCN and the reflection probability far exceeds the corresponding values for the best supermirrors available [15] . Thus nanoparticle reflector bridges the energy gap between efficient reactor reflectors for thermal and cold neutrons, and the effective Fermi potential for UCN. This phenomenon has a number of applications. Such a reflector can be used for VCN and UCN sources, for the more efficient guiding of VCN and, probably, of even faster neutrons at “quasi-specula” trajectories.

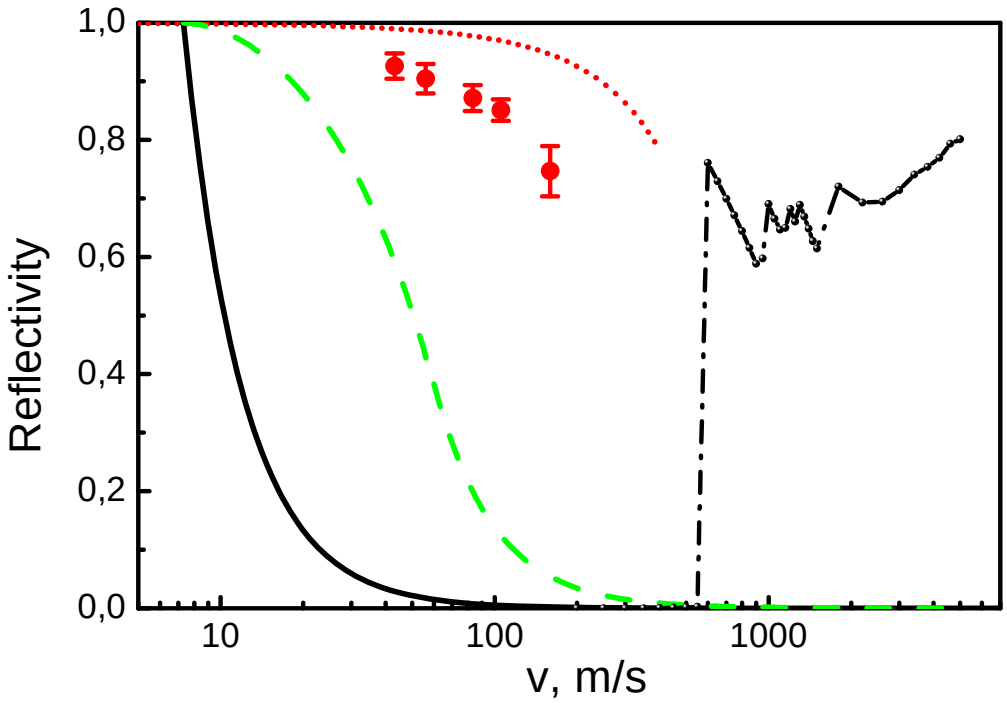


Fig. 10. The elastic reflection probability for isotropic neutron flux is shown as a function of the neutron velocity for various carbon-based reflectors: 1) Diamond-like coating (DLC) (thin solid line). 2) The best supermirror [15] (dashed line). 3) Hydrogen-free ultradiamond [16] powder with the infinite thickness (dotted line). Calculation. 4) VCN reflection from ~3 cm thick diamond nanopowder at room temperature (points), with significant hydrogen contamination [this paper]. Experiment. 5) MCNP calculation for reactor graphite reflector [17] at room temperature with the infinite thickness.

## References


1 V.V.Nesvizhevsky E.V.Lychagin, A.Y.Muzychka, A.V.Strelkov, G.Pignol and K.V.Protasov “The reflection of very cold neutrons from diamond powder nanoparticles,”// Nucl. Instrum. Meth. A **595**, 631 (2008).

2 E.Fermi, “A course in neutron physics" in "Collected papers”, The University of Chicago Press, Chicago (1965).

3 V.I.Luschikov, Yu.N.Pokotilovsky, A.V.Strelkov and F.L.Shapiro, JETP Lett. **9** (1), 23-26 (1969).

4 V.V.Nesvizhevsky, "Interaction of neutrons with nano-particles" // Phys. At. Nucl. **65**, 400 (2002). [Yad. Fiz. **65**, 426 (2002)].

5 P.J.De Carli and J.C. Jamieson, Formation of Diamond by Explosive Shock Science **133**, 1821 (1961).

6 A.E.Aleksenskii, M.V.Baidakova, A.Y.Vul' and V.I.Siklitskii, “The structure of diamond nanoclusters.” // Physics of Solid State **41**, 668 (1999).

7 V.Yu.Dolmatov, “Detonation-synthesis nanodiamond: synthesis, structure, properties and applications” // Russian Chemistry Review **76**, 339 (2007).

8 A.Steyerl and W.-D.Trüstedt, “Experiments with a neutron bottle” // Z.Physik **267**, 379 (1974).

9 S.S.Arzumanov, L.N.Bondarenko, P.Geltenbort, V.I.Morozov, Yu.N.Panin, “Cold-Neutron Storage Owing to Diffusion Reflection” // Phys. At. Nucl. **68**, 1141 (2005).

10 V.V.Nesvizhevsky, G.Pignol and K.V.Protasov, “Nanoparticles as a possible moderator for an ultracold neutron source.” IJN **6** (6), 485 (2007).

11 V.A.Artem'ev, “Estimation of neutron reflection from nanodispersed materials” // Atomic Energy **101**, 901 (2006).

12 V.K.Ignatovich, "The Physics of Ultracold Neutrons", Oxford University Press (1990) ISBN 0198510152

13 R.Golub, D.Richardson and S.K.Lamoreaux, "Ultra-Cold Neutrons", Adam Higler (1991). ISBN 0 7503 0115 5

14 A.L.Vereschagin, G.V.Sakovich, V.F.Komarov, and E.A.Petrov, "Properties of ultrafine diamond clusters from detonation synthesis." // Diamond and Related Materials **3**, 160 (1993).

15 R. Maruyama, et al., Thin Solid Films 515 (2007) 5704

16 http://www.ultradiamondtech.com

17 E. Fermi, *“A course in neutron physics” in “Collected papers”* (The University of Chicago Press, Chicago, 1965).